BOUNDARY SOURCES OF POTENTIAL VORTICITY IN GEOPHYSICAL CIRCULATIONS

ROBERT HALLBERG
NOAA Geophysical Fluid Dynamics Laboratory
Box 308, Princeton, NJ 08542
PETER B. RHINES
University of Washington, School of Oceanography
Box 357940, Seattle, WA 98195

The global ocean is so heavily density-stratified that forcing is mostly restricted to lie at or near its top and bottom boundaries. The general circulation is determined by mass, heat and momentum exchange with the atmosphere and the solid Earth. The primary conservible tracers, potential vorticity (PV) and potential density, are also forced at these boundaries, and yet it is difficult to assess the rate of PV influx from the other, more 'natural' boundary conditions. Here we argue that intersection of surfaces of constant potential density with the boundaries provides reservoirs of large PV, which can be tapped by the circulation. We concentrate on the bottom source, and use a new isopycnal numerical model to examine it. The sloping bottom of the ocean produces a broad region of PV reservoir, and it promotes significant change in both the interior general circulation and the structure of western boundary currents.

Numerical simulations are described which suggest that the PV of the wind-driven circulation is strongly conditioned by passage through boundary currents (and their PV reservoirs), which tends to compete with interior eddy mixing of PV in determination of the mean internal value of PV.

1. Introduction

The generation and decay of vorticity near fluid boundaries is an important and sometimes surprising aspect of classical fluid dynamics (e.g., Morton, 1984). The no-slip condition and pressure gradient tangent to the boundary are strongly involved, as is separation of the outer flow from the boundary. Lift and induced drag are expressed through this vorticity production, being proportional to the equal and opposite net circulation bound to a lifting body. In stratified fluids the strong shedding of atmospheric vortices by mountains and islands (visible as nearly horizontal circulations with lateral scale of kilometers or more) have recently been analyzed using basic potential vorticity (PV-) theory (Schär and Smith, 1993b; Schär and Durran, 1997). A homogeneous rotating fluid provides a large planetary vorticity which can be tapped by

R.M. Kerr and Y. Kimura (eds.), IUTAM Symposium on Developments in Geophysical Turbulence, 51–65.

flows over topographic features: typically, large rest-state PV is swept off the tops of ridges or seamounts, and this produces positive relative vorticity downstream: a force bearing circulation akin to the starting vortex/bound vortex pair described above.

In the large-scale oceanic general circulation the PV involves strong stratification of potential density, Coriolis forces, and spherical Earth (due to the meridional gradient of the Coriolis parameter) effects. PV, defined as

$$q = (f + \hat{\boldsymbol{k}} \cdot \nabla \times \boldsymbol{u})/h \tag{1}$$

for a thin shell on a spherical Earth, is materially conserved for inviscid, adiabatic flow. In (1), f is the vertical component of the Earth's rotation vector, $\boldsymbol{u}$ is horizontal velocity, and h is either the thickness of a layer bounded by two surfaces of constant density ('isopycnals') or the total depth of the ocean (in the case of unstratified fluid). Inviscid, steady flow must go along contours of constant PV, and gradients of PV along isopycnals figure prominently in the dynamics of the large scale ocean circulation.

1.1. THE PV DYNAMICS OF THE WIND DRIVEN OCEAN CIRCULATION

The classic description of the westward intensified barotropic wind-driven ocean circulation, originally due to Stommel (1948), can be made quite clearly in terms of PV conservation (Pedlosky, 1987). In Stommel's barotropic, flat-bottomed model the wind stress curl in the ocean's interior imparts PV to fluid columns. This change in PV is largely manifest as changes in the planetary vorticity in northward (in the subtropical gyre) or southward flow (in the subpolar gyre) (Sverdrup, 1947). In steady state the integral of PV forcing in a region bounded by closed streamlines must be zero, so some other forcing of PV must balance the wind stress forcing. In Stommel's model viscosity acting on the relative vorticity in the western boundary current provides this balance.

When sloping bathymetry is included, the interior PV contours are given by isopleths of f/H, where H is the total depth of the ocean. Streamlines are driven across these contours by the wind stress curl, and this forcing must still be balanced by (viscous) forces of the opposite sign, but the viscous boundary layers can be quite small, limited to the equatorial western boundaries (Salmon, 1992).

The same constraint holds for flow in any isopycnal layer in a stratified ocean. If the time mean streamlines cross time mean layer PV contours due to vortex forcing, there must be balancing vortex forcing of the opposite sign. But in the case of stratified fluid, the PV contours are strongly influenced by the dynamically malleable stratification, rather than just the preordained basin geometry.

Subsurface isopycnal layers are shielded by overlying stratification from the vortex forcing by the wind stress, and viscous processes are thought to be quite weak in the interior, so it is traditionally assumed that mean streamlines coincide with mean PV isopleths. Luyten et al. (1983) note that there cannot be flow along PV contours that intersect the eastern boundary, while PV contours that outcrop may have substantial wind driven flow along them. Rhines and Young (1982) have found that if eddy stirring is able to create regions of closed PV contours, there can be significant mean flow along streamlines that coincide with the closed PV contours, and the planetary geostrophic dynamics of the interior ocean do seem to encourage the formation of such

regions. Since PV is materially conserved, Rhines and Young (1982) further argue that eddy stirring with the closed PV contours should tend to homogenize PV within these regions, in which case the large-scale mean flow can be calculated completely from the thermal wind equations.

The prospect of homogenized circulation gyres makes it plausible that the PV burden involved in major meridional excursions of the fluid can be largely relieved, without the necessity for the level of dissipation seen in homogeneous-density ocean models. Boundary currents could then more nearly conserve PV than dissipate it. One still must balance the circuit integral of the wind-stress with dissipation, but this can be achieved in deep layers to which horizontal momentum is transported by eddy form drag (corresponding to lateral PV flux by eddies, which can then exchange PV with a surface reservoir of high PV).

Haynes and McIntyre (1987) have demonstrated that the PV integrated vertically and horizontally through isopycnal layer only changes due to boundary stresses. This statement is in some ways a mathematical tautology - after all the PV integrated vertically through a layer is just the absolute vorticity on an isopycnal surface. The time evolution of absolute vorticity is given by the curl of the momentum equations, so a horizontal integral of this equation can always be written as a path integral around the boundary from Stokes theorem.

There is no such constraint on the integral of squared PV, potential enstrophy. Since PV is materially conserved for inviscid, adiabatic flow, all of its higher moments, including potential enstrophy, are conserved as well under the same constraints. But potential enstrophy tends to be dominated by very short spatial scales, which are susceptible to viscous dissipation. In essentially two-dimensional geostrophic turbulence, the simultaneous conservation of total energy and potential enstrophy tends to cause the energy to cascade to large scales while the potential enstrophy cascades to small scales (e.g., Salmon, 1998). When the viscosity is sufficiently weak not to cause rapid spindown of energy but strong enough to erode potential enstrophy, there is a tendency for geostrophic turbulence to evolve towards the minimum potential enstrophy state (with homogeneous PV) which is consistent with the given level of total energy, and then towards a minimum potential energy state as the fluid cascades from baroclinic toward barotropic eddy states (Rhines, 1979). This state is also the statistical mechanical equilibrium state of inviscid unstratified geostrophic turbulence (Eby and Holloway, 1994). In a flat-bottomed unstratified ocean, this state is the well known solution of Fofonoff (1954).

But viscosity can also act to increase potential enstrophy. The rest state has significant PV gradients to the planetary vorticity gradient. There is significant available potential energy associated with a state of homogeneous PV (and minimum potential enstrophy). As energy is drained from a flow in statistical equilibrium, potential enstrophy is increased. A similar viscous dishomogenization of PV plays a critical role in the development of a wake in the lee of flow over isolated mountains (Schär and Smith, 1993a).

1.2. BOUNDARY CONTRIBUTIONS TO STRATIFIED POTENTIAL VORTICITY

The ocean is bounded by its free surface, where fluxes of momentum, mass and buoyancy occur, and its bottom, with a thin turbulent boundary layer. Isopycnals intersect the surface and bottom: both because the seafloor slopes, and because the vertically sheared geostrophic circulation is balanced by sloping isopycnal surfaces, there are significant intersections of isopycnals and boundary slopes.

These intersections represent reservoirs of large PV. The wedge-shaped regions of intersection in a layered-density model show this explicitly, and in the limit of continuous stratification, we have delta-function sheets of PV first described by Bretherton (1966) for horizontal boundaries intersected by tilted sigma surfaces and by Rhines (1979) for generally tilted boundaries, in the quasi-geostrophic equations. In the latter case the PV sheets unify the description of topographic and Rossby waves, wave/mean-flow interaction, and instability, all of which are dependent upon gradients of mean PV. With few direct sources of PV in their interior, the oceans are particularly dependent on injection from top and bottom. Given that the PV field encodes much of the velocity field and perturbation mass field, this injection can affect the entire structure of the general circulation.

Such plumes of high PV magnitude have been seen in finite-amplitude Eady-model baroclinic instability calculations (Nakamura and Held, 1989; Garner, Nakamura and Held, 1992), where they can interact much as in the 'roll-up' of a classical two-dimensional vortex sheet. In these calculations one begins with a fluid whose PV is constant, and the plumes of high PV entering from the boundaries act to equilibrate the growing baroclinic waves. Here, we describe the occurrence of similar plumes of high PV magnitude in isopycnal numerical simulations of the ocean circulation.

In an adiabatic fluid, these plumes of high PV magnitude are also accompanied by a reduction of the PV of fluid elsewhere, or by decreasing density gradients at solid boundaries, as in the case of the Eady problem (these two possibilities are equivalent in the Bretherton (1966) description). The PV of a material fluid parcel is only changed by the curl of viscous stresses or by diabatic forcing, and an interior viscous stress will typically contribute regions of both positive and negative curl, often quite close to one another. These plumes, and the viscous interactions between eddies and topography that create them, can be considered an eddy source of potential enstrophy for the interior. This source of potential enstrophy competes with the tendency for interior eddy stirring to homogenize PV and dissipate potential enstrophy. While the mean PV structure, and not the level of potential enstrophy, is of primary interest in this discussion, the processes that create and destroy potential enstrophy are closely tied to the maintenance of the mean PV structure of the statistically steady circulation.

Stommel and Arons (1972) have noted the tendency for conservation of PV to lead to very broad deep western boundary currents over sloping topography, with isopycnal surfaces nearly parallel to the bottom topography. Such structures are, in fact, widely observed. Here we suggest that eddy-topography interactions may create very similar boundary current structures even without a net transport of watermasses.

The sloping-bottom contribution of PV to the interior ocean circulation is examined here with eddy permitting numerical simulations. These simulations use sufficiently

high resolution both in the horizontal and in density to resolve the interaction between interior isopycnals and the bottom. Numerical models based on isopycnal layers rather than Cartesian levels, such as the one used here, are particularly suited to this work, owing to the conservation properties within layers, which accord with the strongly isopycnal nature of conservation in the real oceans.

2. Description of Experiments

This manuscript describes a series of numerical experiments using the isopycnal-coordinate ocean model of Hallberg (1995). The momentum equations are solved as

$$\frac{\partial \boldsymbol{u}_n}{\partial t} + \left[\frac{f + \hat{\boldsymbol{k}} \cdot (\nabla_\rho \times \boldsymbol{u}_n)}{h_n}\right] \hat{\boldsymbol{k}} \times (h_n \boldsymbol{u}_n) \tag{2}$$

$$= -\nabla_\rho \sum_{j=1}^{n} \left[g'_{j-1/2} \left(-D + \sum_{k=N}^{j} h_k \right) \right] - \nabla_\rho \frac{1}{2} (\boldsymbol{u}_n \cdot \boldsymbol{u}_n)$$

$$- \frac{1}{h_n} \nabla_\rho \cdot [A h_n \nabla_\rho (\nabla_\rho^2 \boldsymbol{u}_n)] + \frac{[\tau_{n-1/2} - \tau_{n+1/2}]}{h_n \rho_0}$$

while the layer continuity equations are

$$\frac{\partial h_n}{\partial t} + \nabla_\rho \cdot (h_n \boldsymbol{u}_n) = 0 . \tag{3}$$

Here $\boldsymbol{u}_n$ is the horizontal velocity of a layer, h_n is the thickness of that layer, $g'_{n+1/2} = g(\rho_n - \rho_{n+1})/\rho_0$ is the reduced gravity across the interface between layers n and n+1 (n increases downward), and $\tau_{n+1/2}$ is the stress across the same interface. The biharmonic along-isopycnal viscosity, A, is set to 1.2×10^{12} m^4 s^{-1} in all of the runs presented here. The gradients, ∇_ρ, are evaluated along isopycnal surfaces. The vertical stress across interior interfaces is defined in a way that is consistent with

$$\tau_{n+1/2} = \nu_{n+1/2} \left[\frac{\partial \rho}{\partial z} \frac{\partial \boldsymbol{u}}{\partial \rho} \right]_{n+1/2} , \tag{4}$$

where ν is a vertically varying viscosity, ranging smoothly in value from 10^{-2} m^2 s^{-1} within 20 m of the surface and 10^{-3} m^2 s^{-1} within 10 m of the bottom to 10^{-5} m^2 s^{-1} in the interior. The wind stress is applied as a stress boundary condition, and a no slip bottom boundary condition is used.

The numerical discretizations in this model exactly conserve the total mass of each layer, and PV is materially conserved apart from the viscous forcing terms. Total energy and potential enstrophy are conserved in the limit of nondivergent flow (Arakawa and Hsu, 1990), again apart from the viscous terms.

The simulations described here use 20 isopycnal layers with a horizontal resolution of 1/4° in a spherical domain. The physical domain extends from the Equator to 40N latitude, and 45 degrees of longitude, giving an average horizontal resolution of 25 km. This makes the simulation marginally eddy-resolving, allowing the graver modes of baroclinic instability yet suppressing the enstrophy cascade to smaller scale. The

vertical resolution is sufficiently high that all of the features discussed here are resolved by more than one layer. Much higher vertical resolution would likely give comparable results, and other simulations with many fewer layers are qualitatively similar.

Four different configurations of the sea-floor are taken for comparison: a 4km deep ocean with flat bottom and vertical sidewalls, and a 4 km deep ocean with continental rises with slopes of 0.004, 0.002, and 0.001 at the western side. The actual hypsometry of the oceans involves many margins steeper than this (bottom slopes exceeding 1%), but also many with these magnitudes. For reasons of limited numerical resolution, the Rossby deformation radius is about 75 km, somewhat larger than in nature, and this helps to justify the wider-than-natural bottom slopes. The wind-driven circulation in the upper 800m sees continental slope widths ranging from 200 km to 600 km.

The wind stress is zonally uniform and purely zonal. The idealized pattern is chosen to have zero stress and zero curl at 40N and 15N and with a maximum magnitude twice as that large as observed in the Atlantic, to compensate for the width of the basin, which is roughly half as wide as the Atlantic.

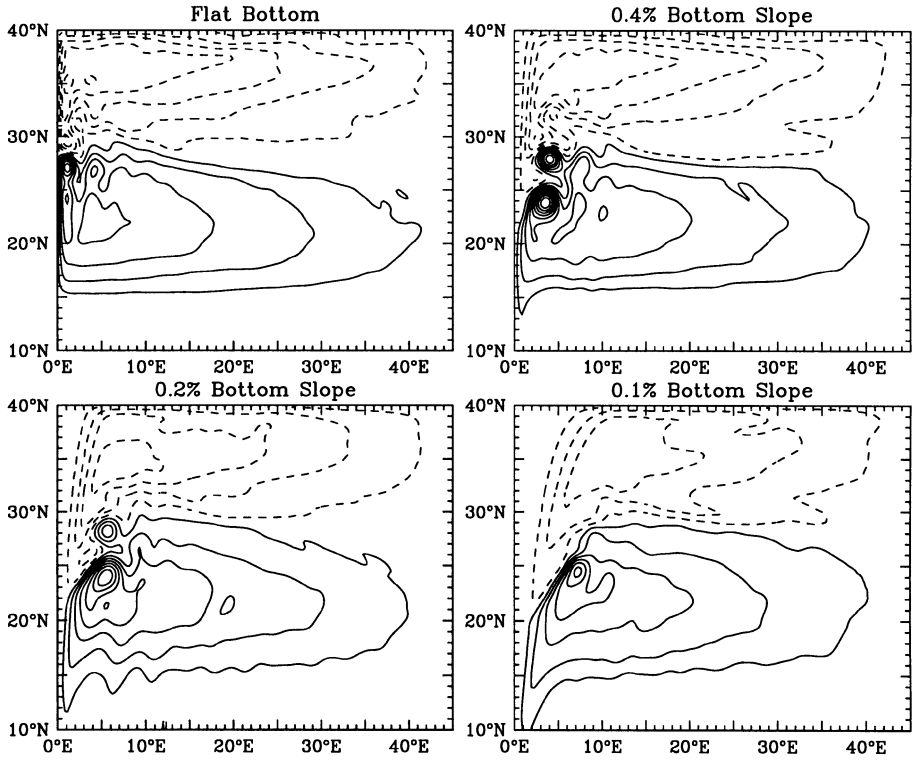

Figure 1. Time mean streamfunction pattern for the depth-integrated circulation in the flat-bottom (top left), 0.4% slope (top right), 0.2% slope (bottom left), and 0.1% slope (bottom right) cases at statistical equilibrium. Cyclonic streamlines are dashed, anticyclonic streamlines are solid and the contour interval is 5×10^6 m^3 s^{-1}. The northern (subpolar) circulation gyre extends southward in a "sleeve" along the slope to an increasing extent with an increasingly gentle slope due to topographic wave dynamics.

3. Effects of Sloping Western Boundary Topography on the Large-scale Flow

The simulations are driven by idealized zonal wind-stress, which produces a familiar Sverdrup/Stommel depth averaged circulation in the form of subpolar and subtropical horizontal gyres with western boundary currents (Fig. 1). Comparison of the flat- and slope- cases shows that the slope shifts the boundary current separation equatorward, while the interior depth-integrated circulation is governed by the Sverdrup (1947) balance and is quite similar between the simulations.

Outcropping layers have a PV balance in which the wind stress figures prominently; the net PV imparted by the wind stress in the outcropping regions must be balanced by frictional effects in the western boundary region. The western boundary layers in these simulations are largely inertial, especially with a sloping bottom. The slope reshapes the western boundary layers (Fig. 2), broadening them, and broader boundary currents are less susceptible to the biharmonic along-isopycnal viscosity used in these simulations. But the PV imparted by the wind stress curl must still be dissipated, and

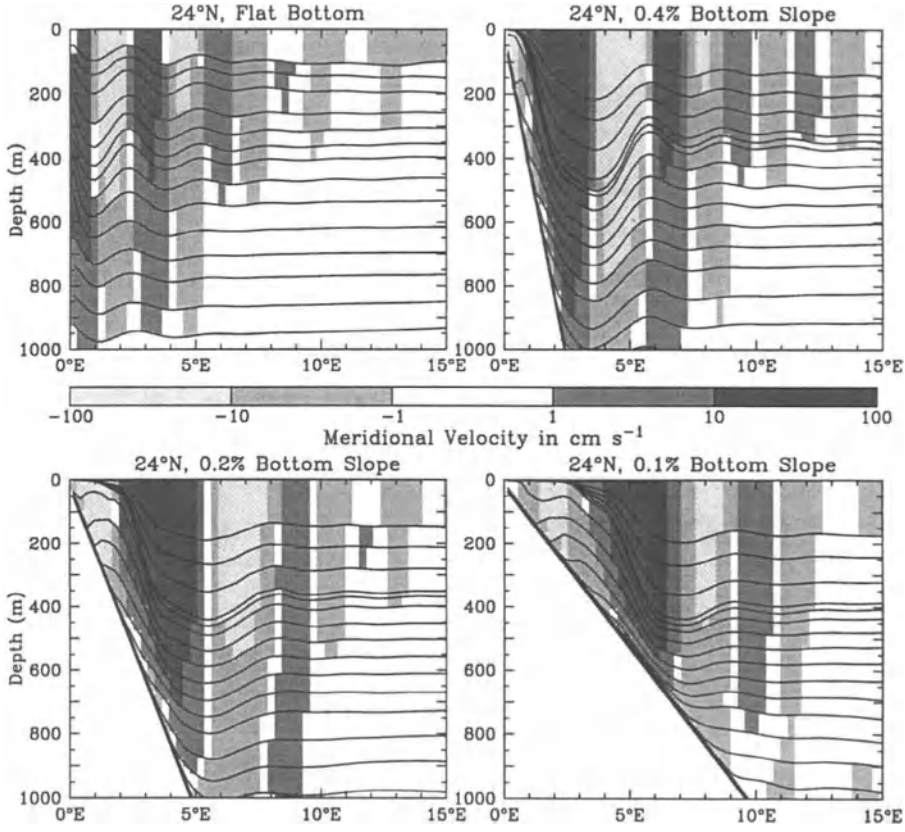

Figure 2. Time mean northward velocity (shaded) and the time mean isopycnal surfaces (lines) on a zonal cross section at 24 N in the western boundary current region of the four simulations

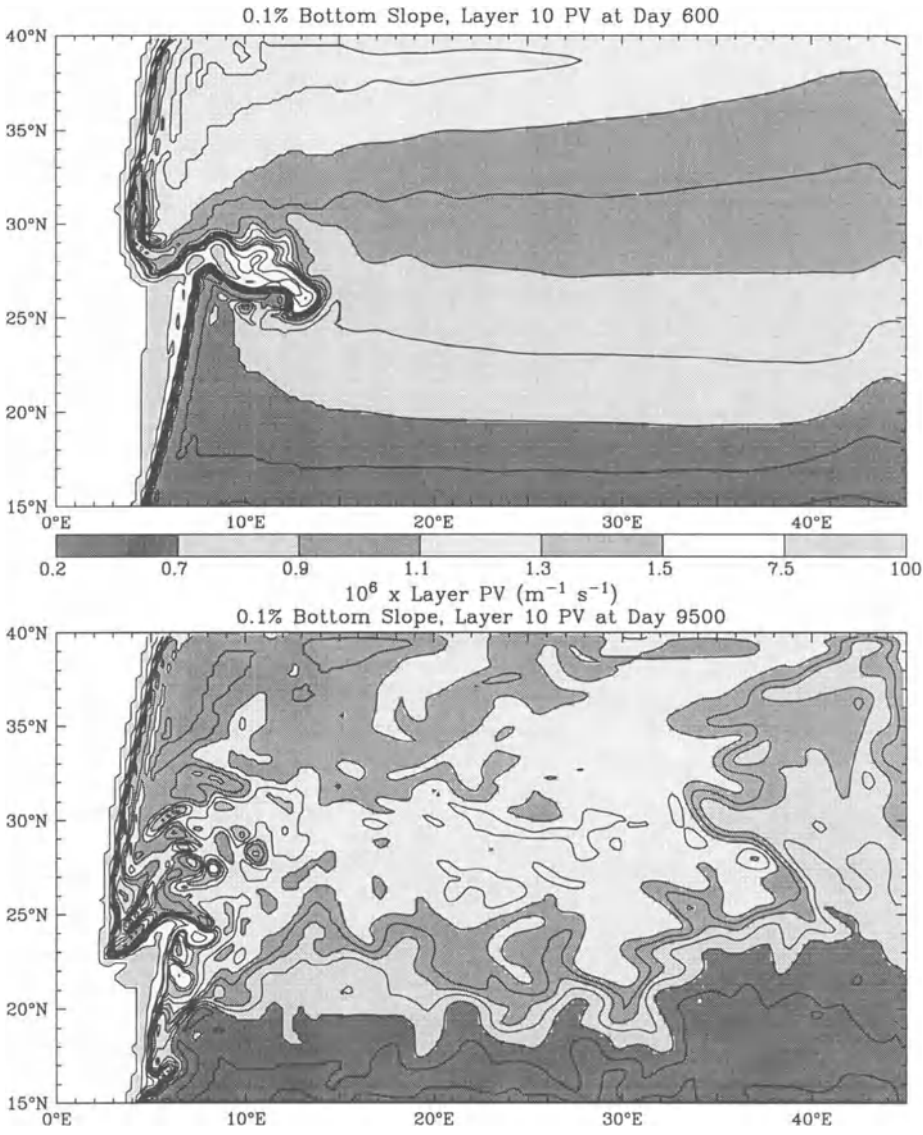

Figure 3. Instantaneous PV of layer 10 (about 600 m deep) in the case with a 0.1% slope at day 600, during the spin-up of the circulation (top), and at day 9500, after a statistically steady state has been reached (bottom). A tongue of cyclonic PV fluid emanates from the western boundary region, and mixes in the interior with anticyclonic PV fluid both from the south and from just offshore of the western boundary. At day 600 the boundary PV source enters at the flow-separation point on the western boundary. Despite strong eddy activity at day 9000, inflow of high PV is still apparent from the west, and this tongue feeds a gentle ridge of cyclonic PV which extends all the way across the basin. The ambient planetary gradient of PV is still visible along the eastern boundary at both times. While the PV tongues are more dramatic with this gentle boundary slope, similar structures occur in the other simulations with sloping boundaries.

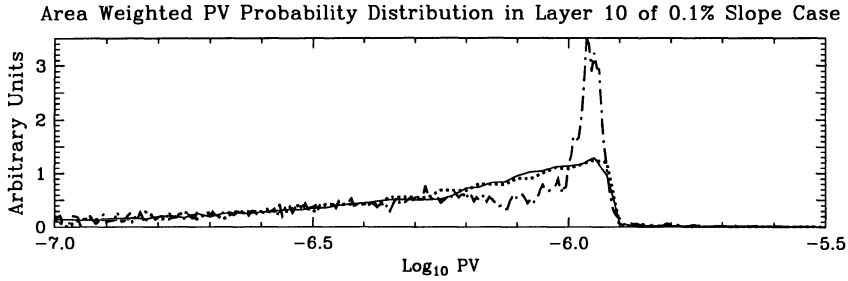

Figure 4. Histogram of PV initially (dotted line), at day 600, during the spin-up of the circulation (solid line), and at day 10000, after a statistically steady state has been attained (dashed-dotted line) for layer 10 of the case with a 0.1% slope. The initially broad distribution describes the latitude-range of the basin, the distribution does not change appreciably in the early spinup, but later this concentrates into a narrow, nearly homogenized PV with larger values reflecting the influence of the bottom boundary high PV sources.

that dissipation occurs both through vigorous eddy mixing between the gyres in the western boundary current separation region and in the strong, recirculation gyres in the mean flow field (Fig. 1). These recirculation gyres are highly reminiscent of those described for a steady, barotropic gyre by Cessi (1991), but in the simulations these recirculation gyres only appear in the time mean, although there are often intense eddies of the appropriate sign in the vicinity of these recirculation gyres.

The less dense layers are generally expelled from the subpolar gyre, so eddies cannot mix fluid with opposing PV anomalies across the gyre boundary in these layers. The along-isopycnal biharmonic viscosity is not effective at dissipating the PV imparted by the wind for the same reason. The PV anomaly dissipation in the less dense layers must occur predominantly through the diapycnal viscosity in these simulations. In the layers that outcrop in the subpolar gyre, wind imparted PV anomalies can be dissipated by along-isopycnal mixing with the subsurface fluid in the subtropical gyres, provided that diapycnal viscosity in the subtropical gyre is sufficiently efficient. With a boundary slope, the subpolar gyre actually extends beneath the subtropical gyre, making vertical viscosity especially effective at retarding the relative vorticity and dissipating the PV anomalies imparted by the winds.

Layers which do not outcrop are shielded by the stratification from the direct effect of the winds. But with a western slope, the intermediate water PV does not tend to become homogeneous over time. Eddies strip cyclonic PV from the boundary which blends with sources of anticyclonic PV from low latitude and from offshore, and in doing so controls the baroclinic general circulation of the interior. These tongues of PV emanating from the boundaries compete with the extensive homogenization of PV that occurs within the broad ocean interior (Fig. 4 and Fig. 3). Shortly after the wind is turned on, this is a laminar process of stripping of high-ambient PV from the slopes; later (Fig. 3), in statistically steady state, fluid recycles through the western boundary layer, partially adjusting (through bottom stress) to the slope, and then reissuing into the interior. The initial plume of high PV is quite similar to the tendency of sufficiently strong impulsively started flow past a seamount to sweep an initial Taylor cap of high PV off of the seamount and downstream as a coherent cyclone; by contrast, the later

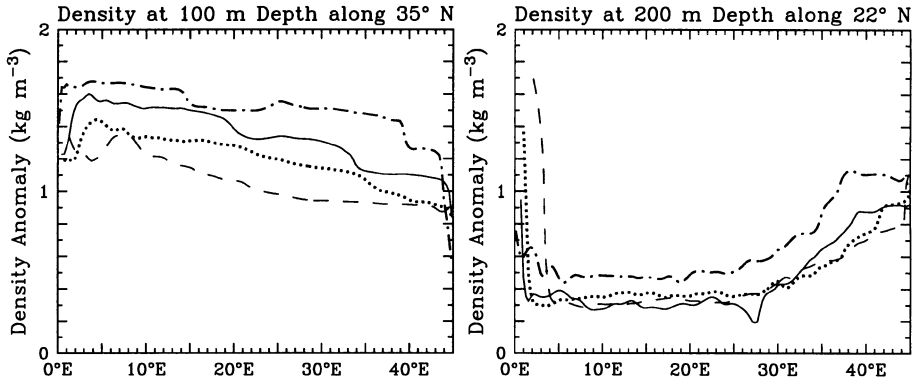

Figure 5. Density anomaly relative to the lightest layer in zonal transects across the subpolar gyre at 35 N at 100 m depth (left) and across the subtropical gyre at 22 N at 200 m depth (right), for the flat bottom case (dashed-dotted line), 0.4% slope (solid line), 0.2% slope (heavy dotted line), and 0.1% slope (dashed line). The density difference between layers is 0.2 kg m^{-3}; these values assume that density varies linearly with depth through each layer. The flat bottom case exhibits much more pronounced doming of isopycnals in the subpolar gyre and a less pronounced isopycnal bowl in the subtropical gyre than do the cases with bottom slopes. Also strongly evident at 22 N is the incursion of dense water up the western slope to an increasing extent with an increasingly gentle slope.

high PV tongue must be continually maintained by viscous processes. In either case the result is a partially homogenized plateau of PV, fed by streams which intermix to set the plateau value.

Generally, a sloping western bottom deepens the northern, subpolar gyre and confines the southern, subtropical gyre to a smaller depth range beneath the surface. This is evident in the streamfunctions of isopycnal layers (not shown), and is closely related through the thermal wind equation to the zonal density structures shown in Fig. 2. With a strongly exaggerated bottom slope, the flow in the subsurface layers is almost all a part of the subpolar gyre, which is pulled equatorward by the 'topographic-wave thrust' along the slope. As a consequence of the deepened, more barotropic subpolar circulation, there is less 'doming' and outcropping of subpolar density surfaces (Fig. 5). With a narrower continental rise, the asymmetry between subpolar and subtropical gyres is less extreme, but still significant. The southward 'push' of the near boundary fluid is especially intense during transient events: to be felt, the sloping boundary must communicate with the water column above, often through eddy activity. In other experiments where the eddies were suppressed, the deep PV tongues were not found, and the circulation was quite similar to the flat bottom case. The vertical structure of the transport is greatly altered by eddies interacting with even the narrow continental slope, which seems to promote broadened, less dissipative boundary currents.

The tongue of high PV in the subsurface layers essentially dictates that these layers must flow almost exclusively in the sense of the subpolar gyre. The PV along the eastern boundary is essentially fixed by the boundary waves leveling all the isopycnals along the boundary, as are values of PV on wave characteristics which emanate from the eastern boundary (Luyten et al., 1982). If the tongue of high PV were to be drawn

southward by flow in the sense of the subtropical gyre, it would lead to very large PV gradients in the eastern part of the domain. The resulting large thermal wind shears would be inconsistent with the generally weak flow in the abyssal interior ocean. Instead, the northeastward deep flow draws the high PV plume to the northern boundary where it essentially matches the ambient PV.

Even with the narrower slope, the western boundary current separation point is significantly equatorward of the zero wind stress curl line (at 23 N, rather than 27.5 N, see Fig. 1). The ocean's western boundary currents all separate equatorward of the zero wind stress curl line, but without invoking topographic influences it has proven difficult to explain this early separation. With quasigeostrophic models topography is limited to the thickness of the bottommost layers, and in many cases stratification shields the wind driven circulation from the topography (Anderson and Killworth, 1978; Thompson 1995). With the large amplitude topography described here, the western boundary current in each layer is influenced by the topography, either directly or through the influence of isopycnals that rise up over the topographic slope.

4. Dynamic Balances in the Western Boundary Region

The location of the PV sources and sinks responsible for the deep mean PV structure are difficult to determine; these sources and sinks have the fundamentally small scales that are prominent in potential enstrophy balances. The average rate at which fluid has its PV modified past two threshold values is shown in Fig. 6. This quantity is related to the sources of potential enstrophy - it shows where the extreme values of PV are being created - but it avoids the very complicated boundary contributions to potential enstrophy (which is infinite, since it is a single vertical integral of a delta function squared). This is also an Eulerian average of a fundamentally Lagrangian quantity: it shows where parcels were when they undergo a change of PV and while the pattern may suggest the physical processes behind these mechanisms, it cannot fully depict the lifecycles of fluid parcels that are ultimately responsible for the mean PV structure.

The highest PV fluid is created (i.e. fluid with lower PV has its value of PV increased) along the western slope, just at the edge of the mean gyre (Fig. 6). Here the mean flow impinges on the slope, creating anticyclonic relative vorticity through vortex compression, and viscosity acting on this fluid imparts net cyclonic PV. The actual volume of high PV fluid created is quite small - only a net 0.04 Sv is modified to have a PV higher than 1.2×10^{-6} m^{-1} s^{-1} along the western boundary from 31N to 40N in layer 10 of the 0.1% slope simulation (Fig. 6), but this fluid attains a very large PV. Offshore the curl of the mean stress is anticyclonic. (It must be so; since the time mean net stress on the layer goes to zero on the slope where the layer vanishes and becomes very small offshore where the mean shears are small, the curl of this stress must contribute both signs in the western boundary region. The small scale is due in part to the importance of the biharmonic along-isopycnal viscosity in forcing the PV.) The offshore stress curl creates a persistent region of low PV relative to the homogenized interior (Fig. 3 and Fig. 6), at a rate of 0.73 Sv with a PV less than 10^{-6} m^{-1} s^{-1} in the same region as the 0.04 Sv of high PV creation. Very high PV fluid is by definition

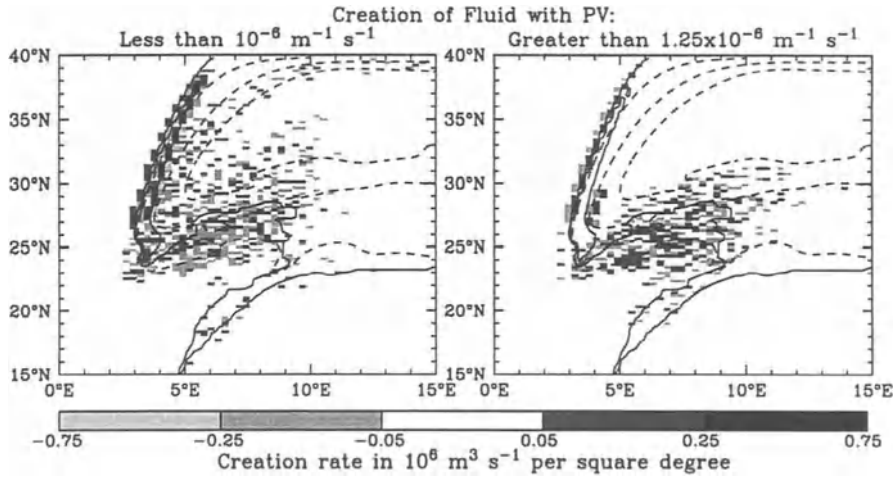

Figure 6. The rate at which fluid with PV lower than 10^{-6} m^{-1} s^{-1} (left) or higher than 1.25×10^{-6} m^{-1} s^{-1} (right) is created in layer 10 of the simulation with a slope of 0.1%. Also shown are the mean streamlines of layer 10 with a contour interval of 0.5 Sv (dashed lines) (1 Sv = 10^6 m^3 s^{-1}); the flow in this layer is all flowing in the cyclonic sense of the subpolar gyre. The location of these PV thresholds in the mean PV fields is also shown (solid lines). The "creation rate" is the rate at which fluid has its PV changed past the threshold value. 101 independent snapshots of the flow were used to assess these creation rates. The threshold PVs were chosen to bracket the values of PV at which the fluid becomes largely homogenized in the interior of the subpolar gyre in this layer. Fluid with a higher PV than the higher threshold occurs in the mean only in the western part of the basin and in a tongue along the separated boundary current. Fluid with a PV lower than the lower threshold occurs in the mean in the southeast corner of this figure and just offshore of the slope in the western portion of the subpolar gyre.

very thin, while low PV is thick, which partially explains this disparity in western boundary layer formation rates. The western boundary patterns of PV forcing are quite robust upon averaging over a few eddy timescales, despite their narrow spatial scales.

The volume of high PV fluid increases dramatically in the separated western boundary current, largely from the mixing of a small amount of very high PV fluid stripped off of the boundary with a large volume of mean or slightly low PV fluid from the interior. The region from 4E to 8.5E and 22.4N to 27N in Fig. 6 encompasses much of the fluid with a mean PV higher than 1.2×10^{-6} m^{-1} s^{-1} in the high PV plume which emanates from the boundary, In this region 0.43 Sv of fluid with a PV higher than 1.2×10^{-6} m^{-1} s^{-1} are created, while 0.49 Sv of fluid with PV less than 10^{-6} m^{-1} s^{-1} are destroyed. In the eastern half of this region 0.05 Sv of fluid with a PV greater than 2x10-6 m-1 s-1 are also destroyed. (These numbers compare with a mean flow of 0.51 Sv through this region.) The high PV fluid is further mixed with lower PV fluid to the east and north of the high PV plume, but it is occasionally occurs well into the interior of the fluid (Fig. 6). Likewise the low PV fluid from near the western boundary is mixed away in sporadic events throughout the western part of the subpolar gyre. In order for fluid with PV greater than a threshold to be created or destroyed, fluid just at that threshold must be subjected to viscous forcing. The fact that the regions where the high and PV fluid is destroyed extend quite far from the mean location of the threshold

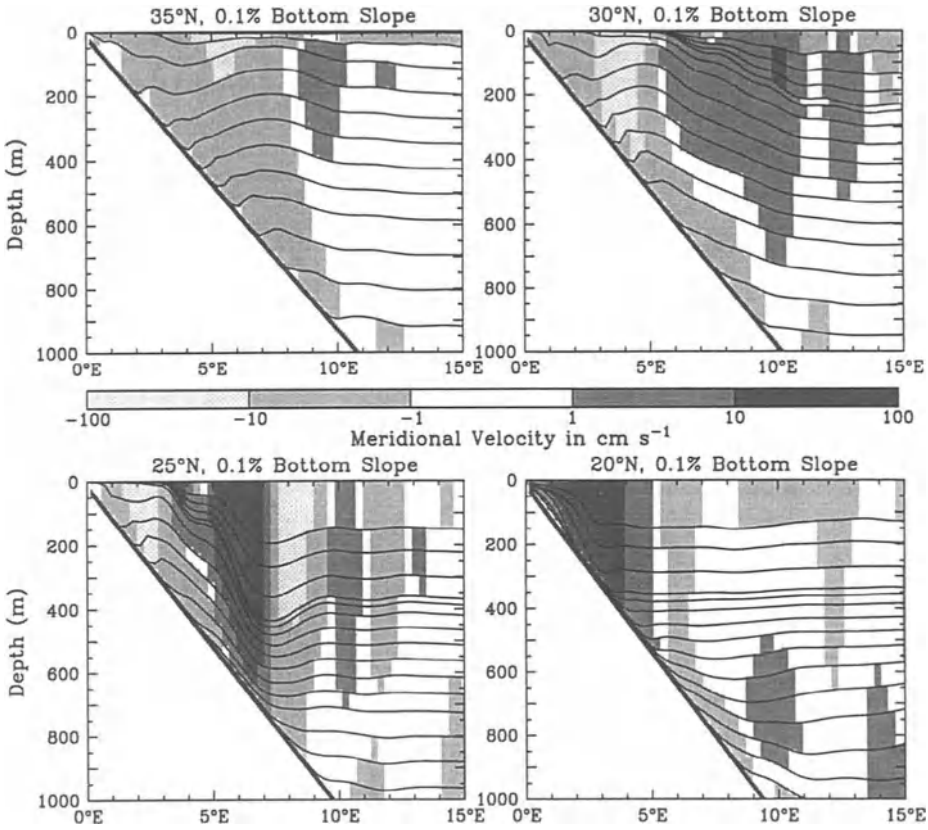

Figure 7. Time mean northward velocity (shaded) and the isopycnal surfaces on a zonal cross section at 35 N, 30 N, 25 N, and 20 N in the western boundary current region of the 0.1% slope case.

PV contour is a strong indication of the importance of eddy transport in the erosion of the high PV tongue.

It is not entirely clear what sets the interior value of the high PV tongue, visible in Fig. 3. Reversed meridional PV gradients, a necessary condition for baroclinic instability, persist well into the fluid, but the baroclinic eddies are apparently unable to completely homogenize the PV in the tongue within the time it takes the fluid to cycle back to the western boundary. It may or may not be a coincidence that the interior PV value in the tongue is nearly equal to the maximum value of PV found on the eastern boundary (Fig. 3), which is essentially the value set by the initial conditions.

A look at the western boundary structure itself provides an alternative description of the processes which are responsible for the subsurface PV structure in these simulations. The well-resolved sloping lower boundary greatly widens the western boundary currents. This realistic baroclinic structure often involves tilted isopycnal surfaces that lie nearly parallel with the bottom, for example beneath the strong northward flowing boundary current (Fig. 7). The associated thermal wind shear

reduces the northward velocity nearly to zero at the bottom and insures that a very weak southward bottom stress is experienced by the northward flow; this is the "slippery bottom slope" of MacCready and Rhines (1993) and Garrett et al. (1994). The slippery bottom slope solution is approached very gradually (the adjustment goes as the square root of time, not exponentially (Garrett et al., 1994)), but the vertical viscosity driving the flow towards this solution tends to create high PV fluid near the bottom beneath the northward flow (even in layers not directly exposed to the bottom). While the slippery bottom slope argument for the existence of the high PV boundary fluid is quite different in flavor from the description in terms of stripping high PV from a boundary reservoir, both are ultimately describing the same viscous processes which modify the PV in the western boundary region and are important in determining the nature of the intermediate depth circulation.

5. Summary

Gradients of density along a solid, non-vertical boundary constitute a potential source of cyclonic PV to a rotating geophysical fluid. This observation has in the past been helpful for describing the evolution of atmospheric instabilities (Schär and Smith, 1993b; Nakamura and Held, 1988). Here we have examined the possible influence of boundary PV due to sloping sides on the large scale ocean circulation.

While the boundary PV source can occur either on a flat ocean bottom or on sloping sides, the ocean's strongly surface intensified flow makes it unlikely that substantial density gradients will occur on the abyssal plains, or that flow there will be sufficiently strong for the interactions with the boundary PV source to influence the large scale flow. The sloping sides of the ocean, though, extend through the large vertical density gradients in the top kilometer of the ocean, and the proximity of intense western boundary currents make interactions with the boundary PV source there potentially important for the dynamics of the large scale ocean circulation. Here we use simulations with a novel density coordinate ocean model that resolves the western boundary slope both vertically and horizontally to explore the effect of the boundary source of high PV from a sloping western boundary on the large scale ocean circulation.

In the simulations presented here, the stripping of high PV off of the sloping western boundary is of equal stature to eddy stirring and homogenization of PV in determining the mean subsurface PV structure. The resulting intermediate depth PV tongue has a dramatic influence on the circulation, dictating that the intermediate water flow is predominantly in the cyclonic sense of the subpolar gyre. The subtropical gyre with a sloping western boundary tends to be strongly surface intensified, while outcropping of dense water in the subpolar gyre is limited. With a sloping western boundary the western boundary current separates equatorward of the zero wind stress curl line, as do western boundary currents in the real world. The boundary sources of PV likely have an important, but as yet only partially understood, role in the dynamics of geophysical circulations.

Acknowledgment

We gratefully acknowledge support of the National Oceanic and Atmospheric Administration, Geophysical Fluid Dynamics Laboratory and the National Science Foundation, Ocean Sciences Division.

References

Anderson, D. L. T., and Killworth, P. D. (1977) Spin-up of a stratified ocean with topography, *Deep-Sea Res.* **22**, 709-732.

Arakawa, A., and Hsu, Y.-J. G. (1990) Energy conserving and potential-enstrophy dissipating schemes for the shallow water equations. *Mon. Wea. Rev.* **118**, 1960-1969.

Bretherton, F. (1966) Critical layer instability in baroclinic flows. *Quart. J. Roy. Meteor. Soc.* **92**, 325-334.

Cessi, P. (1991) Laminar separation of colliding western boundary currents. *J. Mar. Res.*, **49**, 697-717.

Eby, M., and Holloway, G. (1994) Sensitivity of a large-scale ocean model to a parameterization of topographic stress, *J. Phys. Oceanog.* **24**, 2577-2588.

Fofonoff, N. P. (1954) Steady flow in a frictionless homogeneous ocean, *J. Mar. Res.* **13**, 254-262.

Garrett, C., MacCready, P. and Rhines P. (1993) Boundary mixing and arrested Ekman layers: Rotating stratified flow near a sloping boundary, *Ann. Rev. Fluid Mech.* **25**, 291-323.

Garner, S. T., Nakamura, N., and Held, I. M. (1992) Nonlinear equilibration of two-dimensional Eady waves: New perspective, *J. Atmos. Sci.* **49**, 1984-1996.

Hallberg, R. (1995) *Some aspects of the circulation in ocean basins with isopycnals intersecting sloping boundaries*, Ph. D. thesis, University of Washington, 244 pp.

Haynes, P. H. and M. E. McIntyre (1987) On the evolution of vorticity and potential vorticity in the presence of diabatic heating and frictional or other forces, *J. Atmos. Sci.*, **44**, 828-841.

Luyten, J. R., Pedlosky, J. and Stommel, H. (1983) The ventilated thermocline, *J. Phys. Oceanog.* **13**, 292-309.

MacCready, P. and Rhines P. B. (1991) Buoyant inhibition of Ekman transport on a slope and its effect on stratified spin-up, *J. Fluid Mech.***223**, 631-661.

Morton, B. R. (1984) The generation and decay of vorticity, *Geophys. Astrophys. Fl. Dyn.* **28**, 277-308.

Nakamura, N. and Held, I. M. (1989) Nonlinear equilibration of two-dimensional Eady waves *J. Atmos. Sci.* **46**, 3055-3064.

Pedlosky, J. (1987) *Geophysical Fluid Dynamics*, Springer-Verlag, New York, 710 pp.

Rhines, P. B. (1979) Geostrophic turbulence, *Ann. Rev. Fluid Mech.* **11**, 401-441.

Rhines, P. B. and Young, W. R. (1982) A theory of the wind-driven circulation. I. Mid-Ocean Gyres, *J. Mar. Res.* **40** (Suppl.), 559-596.

Salmon, R. (1992) A two-layer Gulf Stream over a continental slope, *J. Mar. Res.* **50**, 341-365.

Salmon, R. (1998) *Lectures on Geophysical Fluid Dynamics*, Oxford University Press, Oxford, 378 pp.

Schär, C. and Durran, D. R. (1997) Vortex formation and vortex shedding in continuously stratified flows past isolated topography, *J. Atmos. Sci.* **54**, 534-554.

Schär, C. and Smith, R. B. (1993a) Shallow-water flow past isolated topography. Part I: Vorticity production and wake formation, *J. Atmos. Sci.* **50**, 1373-1400.

Schär, C. and Smith, R. B. (1993b) Shallow-water flow past isolated topography. Part II: Transition to vortex shedding, *J. Atmos. Sci.* **50**, 1401-1412.

Stommel, H. (1948) The westward intensification of wind-driven ocean currents. *Trans. Amer. Geophys. Union* **29**, 202-206.

Stommel, H. and Arons, A. B. (1972) On the abyssal circulation of the world ocean-V. The influence of bottom slope on the broadening of inertial boundary currents, *Deep-Sea Res.* **19**, 707-718.

Sverdrup, H. U. (1947) Wind-driven currents in a baroclinic ocean; with application to the equatorial currents of the Eastern Pacific, *Proc. Nat. Acad. Sci.* **33**, 318-326.

Thompson, L. (1995) The effect of continental rises on the wind-driven ocean circulation, *J. Phys. Oceanog.* **25**, 1296-1316..